Freezing and melting transitions of liquids in mesopores with ink-bottle geometry

2007 New J. Phys. 9 272

(http://iopscience.iop.org/1367-2630/9/8/272)

New Journal of Physics
The open-access journal for physics

Freezing and melting transitions of liquids in mesopores with ink-bottle geometry

Alexey Khokhlov[1], Rustem Valiullin[1,3], Jörg Kärger[1], Frank Steinbach[2] and Armin Feldhoff[2]

[1] Fakultät für Physik und Geowissenschaften, Universität Leipzig, Leipzig 04103, Germany
[2] Institut für Physikalische Chemie und Elektrochemie, Universität Hannover, D-30167 Hannover, Germany
E-mail: khokhlov@uni-leipzig.de, valiullin@uni-leipzig.de, kaerger@physik.uni-leipzig.de, frank.steinbach@pci.uni-hannover.de and armin.feldhoff@pci.uni-hannover.de

New Journal of Physics **9** (2007) 272
Received 14 June 2007
Published 17 August 2007
Online at http://www.njp.org/
doi:10.1088/1367-2630/9/8/272

Abstract. Freezing and melting behavior of nitrobenzene in mesoporous silicon with different pore size and with different porous structure have been studied using ^{1}H NMR cryoporometry. With the bulk phase surrounding the porous monoliths, in materials with uniform channel-like pores distinct pore-size-dependent freezing and melting transitions have been measured. These data were further used for the analysis of the fluid behavior in samples with modulated porous structure, namely linear pores with alternating cross-section. We have, in particular, considered two materials consisting of channel sections, which were separated by almost identical channel 'necks' but notably differed in the respective channel diameters. In the smaller channel segments, the observed shift in the freezing temperature provides direct evidence of the relevance of a pore-blocking mechanism, i.e. of the retardation in the propagation of a solid front by the channel necks. In the channel segments with larger diameter, on the other hand, freezing is found to be initiated by homogeneous nucleation.

[3] Author to whom any correspondence should be addressed.

PII: S1367-2630(07)52764-3

Contents

1. Introduction

It is well documented that phase transitions under confinement are often shifted in comparison with those in the free fluid. Among a variety of such examples, fluid–solid (freezing) and solid–fluid (melting) transitions in nanoporous solids have attracted particular attention [1]–[4]. A very broad spectrum of experimental results obtained using porous materials of various pore sizes, morphologies and types of fluid–solid interaction has greatly promoted the general understanding of these phenomena. However, some aspects still require further experimental and theoretical analysis. This, in particular, concerns the quantification of the freezing/melting hysteresis—namely the phenomenon of diverging melting and freezing transitions [5]–[10].

In classical theories, hysteresis is often associated with the occurrence of different thermodynamical conditions under which these transitions are thought to occur. For example, expressing the total free energy of a fluid in an ideal cylindrical pore as a function of the volume fraction of a frozen core, within a certain temperature range, one finds two local minima in the free energy [8, 11]. These correspond to a liquid-filled pore and a pore with a frozen core, except a few monolayers adjacent to the pore walls. In this approach, it is argued that the freezing condition is found by equating the free energies at the two minima while melting occurs at just this temperature where the latter minimum disappears. Crucially, however, these conditions assume that nucleation, recalling the first-order-character of the transitions, is not a limiting process [12].

For the melting transition in small pores, the latter may be justified by referring to the fact that, in most cases, nuclei of the liquid phase are present at all relevant temperatures. Indeed, the existence of non-frozen surface layers on the pore walls has found much experimental evidence [13], including NMR studies [14]–[16]. In this way, melting in a single pore is often assumed to take place at the equilibrium transition temperature [17]. For the freezing transition, on the other hand, two situations may be envisaged: freezing may be initiated either by nucleation in the pores or by solid-front penetration if the pores are in contact with the bulk-frozen phase [18]–[21]. As experimental evidence for this, one may refer to a substantial dependence of the freezing temperature on pore filling factors [7, 17, 22]. In materials with random porous structure, in both cases, however, the freezing front either growing in the porous matrix or penetrating into the pores may become stuck at the pore constrictions if their dimensions are small enough to provide sufficiently high free energy barriers to overcome. In the literature, this effect is referred to as the pore-blocking (or ink-bottle) effect and is widely assumed to contribute to the freezing/melting hysteresis.

The pore-blocking concept is involved in the rationalization of a number of phenomena such as gas desorption from random pores [23] or mercury intrusion [24]. However, molecular

dynamics simulation studies of adsorption/desorption processes in ink-bottle-shaped pores have revealed that under certain conditions the pore blocking can be bypassed by cavitation, i.e. evaporation from large cavities can occur even if narrow necks remain filled by the liquid [25]. The same scenario emerged from Monte Carlo and density functional theory studies, providing deeper insight into the phenomenon [26, 27]. The availability of well-ordered mesoporous materials with three-dimensional (3D) cage-like structures allowed the experimental validation of the behavior revealed by theoretical analysis and their direct comparison [28]–[31]. Thus, Ravikovitch and Neimark [29, 30] have experimentally verified three possible mechanisms of evaporation from ordered mesoporous materials: (i) evaporation due to cavitation from large enough pores, (ii) pore-blocking-controlled desorption and (iii) near-equilibrium desorption from large pores having direct access to the bulk reservoir.

To our knowledge, there is only one systematic study [32] of freezing in well-ordered materials with a network of ink-bottle pores under pore-blocking control. On changing the size of the cavities and the connecting necks, the authors have observed two distinct regimes of freezing. It was experimentally found that, with a neck size of less than about 4 nm, the pore water in the cavities froze by a mechanism of homogeneous nucleation. With large neck sizes, however, the freezing transition has been found to increase and to broaden, indicating a gradual, percolation-like freezing along the cavities and the necks whose size is sufficiently large to allow the propagation of the ice front.

Benefiting from our ability to produce mesoporous silicon with channel-like pores and varying cross-section, in the present work we are going to follow a suggestion emerging from the studies by Morishige *et al* [32] and experimentally test the relevance of the pore-blocking concept for the freezing transition in specially designed pore architectures. In this way, by means of NMR cryoporometry, we are able to provide direct evidence that, depending on the relation between the sizes of the necks and of the channel segments separated by them, both freezing delayed by pore blocking and freezing by homogeneous nucleation in the larger pores (analogue to cavitation in desorption) can be observed. Moreover, our experimental findings reveal that the character of the freezing process depends on the arrangement and the interconnectivity of the pores with different sizes. Thus, changing these properties provides an interesting option to initiate controllable percolation processes.

2. Experimental section

The porous silicon (PSi) [33, 34] samples have been prepared by electrochemical etching (anodization) of single-crystalline (100)-oriented p-type Si wafers with a resistivity of 2–5 mΩ cm. The electrolyte contained HF (48%) and C_2H_5OH in a ratio of 1:1. Two samples with different pore sizes have been prepared by applying constant current densities $j_1 = 20\,\mathrm{mA\,cm^{-2}}$ (P1) and $j_2 = 80\,\mathrm{mA\,cm^{-2}}$ (P2). In this way, non-intersecting linear pores with pore diameters of about 5.6 and 7.5 nm, respectively, are produced [35]–[37]. A third PSi sample (PM1) has been produced by alternating the current density between j_1 and j_2 with durations chosen to yield equal volumes of the pore sections with different diameters (see the schematic structure in figure 1(a)). A fourth sample (PM2) has been produced in the same way as PM1, with the current density alternated between $j_1 = 20\,\mathrm{mA\,cm^{-2}}$ and $j_3 = 120\,\mathrm{mA\,cm^{-2}}$. Etching steps with larger currents ($j_3 > j_2$) lead to larger pores (of about 10 nm diameter). For removing the PSi films from the substrates, an electropolishing step with a current density of $700\,\mathrm{mA\,cm^{-2}}$ was applied for 2–3 s. In all cases, the total anodization duration has been chosen to provide a

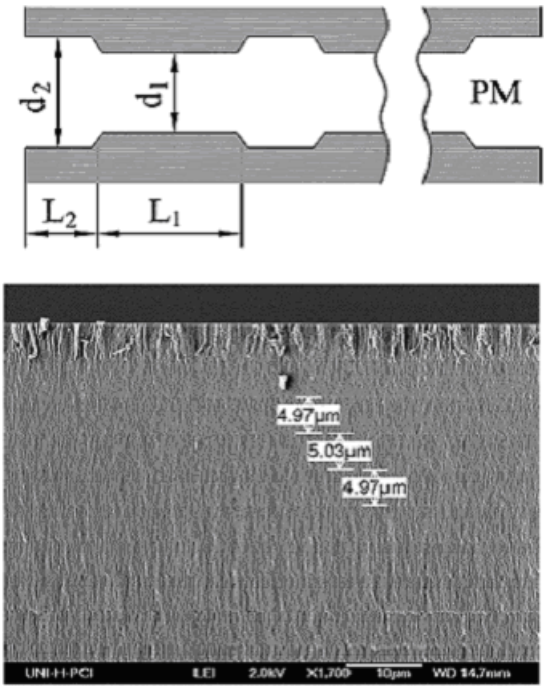

Figure 1. (Top figure) 2D representation of the pore section in the PSi (PM1) obtained by modulation of the anodization current density. The etching parameters were chosen to yield $d_1 = 5.6\,\text{nm}$, $d_2 = 7.5\,\text{nm}$, $L_1 = 3.25\,\mu\text{m}$ and $L_2 = 1.75\,\mu\text{m}$. The PM2 sample had a similar structure, but with $d_1 = 6.2\,\text{nm}$, $d_2 = 10.4\,\text{nm}$, $L_1 = 12.0\,\mu\text{m}$ and $L_2 = 4.0\,\mu\text{m}$. The total thickness of the PSi films was about $50\,\mu\text{m}$ in both cases. (Lower figure) SEM micrograph parallel to the wafer surface displaying a well-defined periodic structure due to the different porosities in the layers.

thickness L of the PSi films of about $50\,\mu\text{m}$. By using scanning electron microscopy (SEM) (figure 1), the real structure of the thus obtained samples has been found to correlate well with the expected one.

To study freezing/melting transitions in the PSi samples, the NMR version [14, 38] of thermoporometry [3, 18] has been employed. This method is based on the fact that the NMR spin–spin relaxation times T_2 in the crystalline (T_2^{crystal}) and the liquid (T_2^{liquid}) phases usually differ by orders of magnitude, viz. $T_2^{\text{crystal}} \ll T_2^{\text{liquid}}$. Under such circumstances, the 90°–τ–180° spin–echo pulse sequence with an inter-pulse delay τ obeying the condition $T_2^{\text{crystal}} < \tau < T_2^{\text{liquid}}$ acts as a filter suppressing the NMR signal from the crystal phase [39]. If, at a certain temperature, the liquid (non-frozen) and crystalline (frozen) phases coexist within the pores, the described procedure yields the NMR signal intensity I of the liquid phase only. Note that I is directly proportional to the number of spin-bearing molecules and, thus, provides a measurable quantity to follow freezing/melting transitions under confinement. In what follows, the thus obtained value of I will be normalized to that measured for pores completely filled with liquid to yield the fraction f of liquid volume in the pores (thus, $f = 0$ refers to pores completely filled with frozen liquid, except for a non-frozen surface layer, and $f = 1$ to completely liquid-filled pores).

The ^{1}H NMR cryoporometry experiments have been carried out on a home-built NMR spectrometer operating at a proton resonance frequency of 400 MHz, equipped with a temperature controller with an accuracy of better than 0.2 K. As a probe liquid, nitrobenzene with the bulk melting temperature $T_m \approx 5.6\,^\circ$C has been used. The PSi crystals placed in the NMR tube have been outgassed and then oversaturated by nitrobenzene. The ^{1}H NMR measurements were performed using the 90°–τ–180° spin–echo pulse sequence with $\tau = 3$ ms. First, temperature has been decreased by small steps (usually 0.5 K). After each step, an equilibration time of about 3 min has been given. Then the spin–echo amplitude has been measured. This was repeated until the NMR signal has almost completely disappeared. Thereafter, the same procedure has been repeated with increasing temperature ('heating branch') until complete signal restoration. The temperature ranges studied correspond to those shown in figures 1–4.

3. Experimental results and discussion

The experimental results shown in figure 2 are the key finding of our work. Figure 2 displays the freezing and the melting transitions of nitrobenzene in three investigated samples. In materials with uniform pores (P1 and P2), relatively sharp melting transitions are observed. The transition temperatures were shifted with respect to the bulk melting point $T_m = 5.6\,^\circ$C and are correlated with the envisaged pore dimensions. This is easily reconciled by referring to the Gibbs–Thompson equation $T_m - T = K/d$ for the melting point T suppression, where K is, in first approximation, a fluid-dependent constant ($K \approx 125$ K nm for nitrobenzene [40, 41]). Most importantly, for the sample PM1 with the modulated structure, the melting curve reveals two transitions with flattening in-between them. The temperature ranges of these two transitions and, hence, the respective pore dimensions correspond well to those for P1 and P2. In addition, the flattening occurs at the half-height of the curve, suggesting equal pore volumes in the sections with the different pore sizes. Thus, the experimental data on melting completely support the structure expected for the sample PM1 owing to the preparation conditions (see figure 1).

The freezing transitions in materials with uniform pores (P1 and P2) appear to be even more strongly suppressed with respect to T_m as compared with the melting transition. Thus, together with the melting branch, well-pronounced, pore-size-dependent hysteresis loops result. Their particular details (shape, width, etc) deserve special assessment and may be left out of consideration in the present context. We are rather interested in the position of the freezing transition in PM1 in relation to those in P1 and P2. If one assumes that freezing in pores proceeds in a qualitatively similar way to melting, i.e. independently in different spatially extended pore sections with different pore sizes, then one would expect the freezing curve for PM1 as shown by the solid line in figure 2. However, the experimentally measured transition is found to be sharp and delayed to the temperatures required to freeze the fluid in the smallest pores (P1).

We anticipate that this observation is the consequence of the pore-blocking effect recalling that our samples contain an extra bulk phase of the liquid surrounding the porous particles. Thus, upon decreasing the temperature below T_m, the bulk phase freezes first at a certain temperature. Upon further cooling, the solid phase cannot ingress into the pores until the thermodynamical conditions favoring the penetration of the solid front into the pore section with diameter d_1 (see figure 1) are fulfilled. It should be noted that this line of reasoning implies that the penetration of a solid front into the pores is the mechanism responsible for pore freezing [18]. In order to clarify this issue, we have performed additional experiments avoiding any bulk phase between the PSi

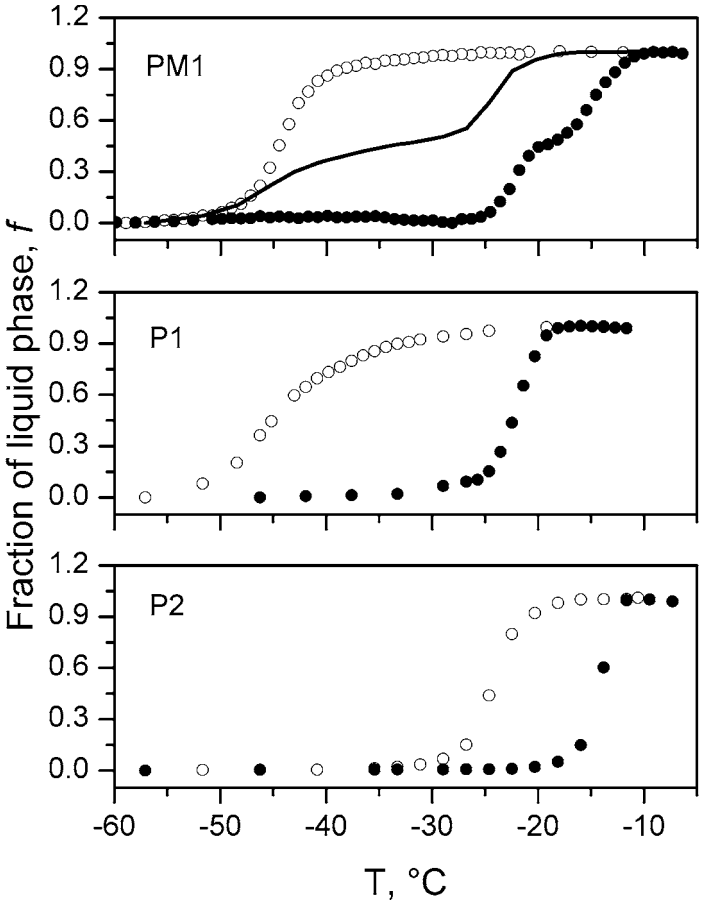

Figure 2. Freezing (open symbols) and melting (filled symbols) transition of nitrobenzene in the PSi samples with channel-like pores with (i) uniform diameters of 5.6 nm (P1) and 7.5 nm (P2) and (ii) diameters alternating between 5.6 and 7.5 nm (PM1). The solid line shows the calculated freezing transition (see explanations in text) for the PM1 sample.

specimens, i.e. the samples have been prepared with complete saturation of the mesoporous space (mesopore filling factor 1) but without any perceptible excess. Figure 3 shows the results for sample P1, as an example. The displayed experimental finding provides clear evidence that the freezing initiated by nucleation within the pores leads to an even stronger suppression of the freezing point than that observed for the sample PM1, being in contact with the bulk phase.

More detailed evidence on the freezing behavior is found with sample PM2. Here, the channels consist of four sections with a diameter of $d_2 = 10.4$ nm, interconnected by narrower channels (necks) with $d_1 = 6.2$ nm (pore sizes determined from the melting transition using the Gibbs–Thompson equation). The two large pores, on each side of the channels, have immediate contact with the bulk fluid. In complete agreement with the above consideration, all these structural features of pore architecture are nicely reflected by the freezing and melting behavior as shown in figure 4. The melting branch exhibits the same pattern as for PM1: one observes two distinct melting transitions corresponding to the melting of nitrobenzene in wider and narrower pores. However, the freezing behavior is quite different from that of the sample PM1 where

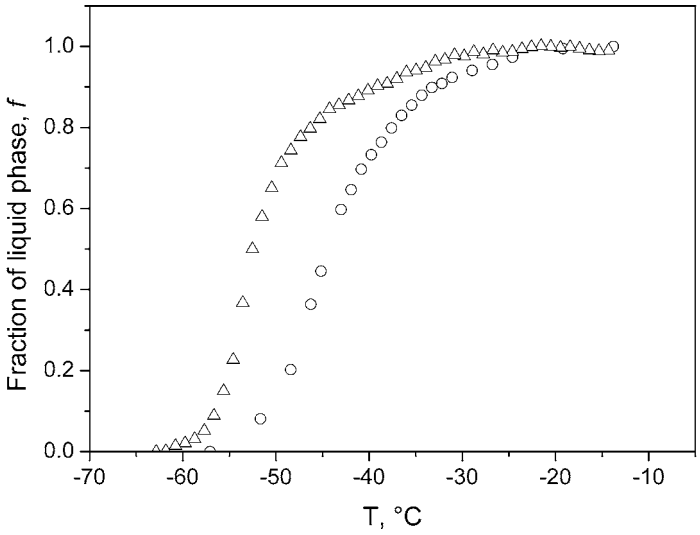

Figure 3. Freezing transition of nitrobenzene in the PSi sample P1 with (open circles, the same as in figure 2) and without (open triangles) a surrounding bulk phase.

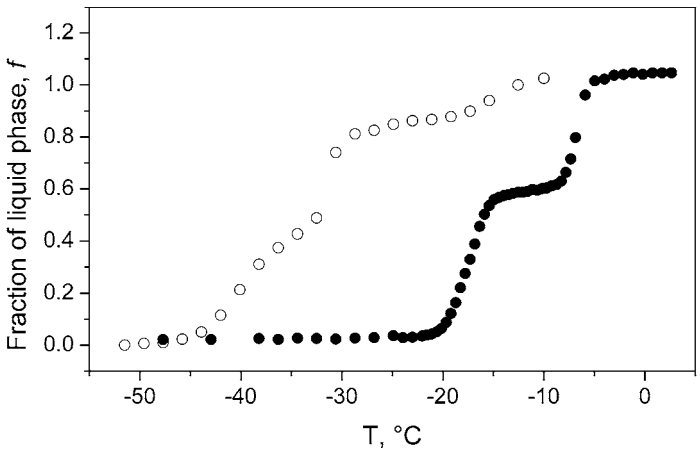

Figure 4. Freezing (open symbols) and melting (filled symbols) transition of nitrobenzene in the PSi sample PM2 with channel-like pores with diameters alternating between 6.2 and 10.4 nm.

the whole of the pore fluid was found to freeze at one temperature, due to pore-blocking control by the narrow pores. Here, two distinct freezing transitions are clearly detected. The first one, taking place at temperatures between −10 and −15 °C, corresponds to the freezing of the fluid in the two wide-channel sections adjacent to the silicon wafer surface, caused by the ingress of a solid front from the bulk frozen phase. Thereafter, the pore-blocking mechanism due to the narrow channels (necks) prevents further ingress of the solid phase. Remarkably, the second freezing transition is detected at a temperature of about −30 °C. In contrast to the sample PM1, where the freezing transition temperature due to the pore blocking is delayed down to −40 °C, in this case the rest of the wide channel sections presumably freeze via

homogeneous nucleation. With further decreasing temperature, a gradual freezing in the narrow-channel sections is observed.

4. Conclusions

In conclusion, we have presented an experimental study of the freezing phenomenon under mesoscalic confinement. Using mesoporous silicon with controllable channel parameters as a model system, we have been able to confirm the relevance of the pore-blocking effect during freezing by solid-front penetration from the outer frozen phase. At the same time, in materials with wider channels separated by necks of the same size, also freezing by homogeneous nucleation is observed. Altogether, with the used samples three different regimes of freezing, similar to that for the desorption from mesoporous cage-like structures [29, 30], are distinguished: (i) freezing due to homogeneous nucleation, (ii) pore-blocking-controlled freezing and (iii) freezing of the large pores having immediate access to the frozen bulk phase. All these effects may be relevant for freezing in materials with random pore structure, where a further growth of the initial crystals nucleated within the pores, or formed in larger pores in contact with bulk solid phase, can be prohibited by the heterogeneity of the structure, e.g. by pore constrictions.

Acknowledgments

We gratefully acknowledge the financial support of this work by the German Science Foundation (DFG), within the frame of the Dutch–German International Research Training Group ‘Diffusion in Porous Media’.

References

[1] Scherer G W 1999 *Cem. Concr. Res.* **29** 1347
[2] Christenson H K 2001 *J. Phys.: Condens. Matter* **13** R95
[3] Landry M R 2005 *Thermochim. Acta* **433** 27
[4] Alba-Simionesco C, Coasne B, Dosseh G, Dudziak G, Gubbins K E, Radhakrishnan R and Sliwinska-Bartkowiak M 2006 *J. Phys.: Condens. Matter* **18** R15
[5] Morishige K and Kawano K 1999 *J. Chem. Phys.* **110** 4867
[6] Faivre C, Bellet D and Dolino G 1999 *Eur. Phys. J.* B **7** 19
[7] Schreiber A, Ketelsen I and Findenegg G H 2001 *Phys. Chem. Chem. Phys.* **3** 1185
[8] Denoyel R and Pellenq R J M 2002 *Langmuir* **18** 2710
[9] Webber B and Dore J 2004 *J. Phys.: Condens. Matter* **16** S5449
[10] Petrov O and Furo I 2006 *Phys. Rev.* E **73** 011608
[11] Unruh K M, Huber T E and Huber C A 1993 *Phys. Rev.* B **48** 9021
[12] Sear R P 2007 *J. Phys.: Condens. Matter* **19** 033101
[13] Dash J G, Rempel A W and Wettlaufer J S 2006 *Rev. Mod. Phys.* **78** 695
[14] Overloop K and Vangerven L 1993 *J. Magn. Reson.* A **101** 179
[15] Stapf S and Kimmich R 1995 *J. Chem. Phys.* **103** 2247
[16] Petrov O V, Vargas-Florencia D and Furo I 2007 *J. Phys. Chem.* B **111** 1574
[17] Wallacher D and Knorr K 2001 *Phys. Rev.* B **63** 104202
[18] Brun M, Lallemand A, Quinson J F and Eyraud C 1977 *Thermochim. Acta* **21** 59
[19] Swainson I P and Schulson E M 2001 *Cem. Concr. Res.* **31** 1821

[20] Soprunyuk V P, Wallacher D, Huber P, Knorr K and Kityk A V 2003 *Phys. Rev.* B **67** 144105
[21] Beurroies I, Denoyel R, Llewellyn P and Rouquerol J 2004 *Thermochim. Acta* **421** 11
[22] Morishige K and Iwasaki H 2003 *Langmuir* **19** 2808
[23] Everett D H 1967 Adsorption hysteresis *The Solid–Gas Interface* ed E A Flood (New York: Marcel Dekker) p 1055
[24] Rigby S P and Fletcher R S 2004 *J. Phys. Chem.* B **108** 4690
[25] Sarkisov L and Monson P A 2001 *Langmuir* **17** 7600
[26] Libby B and Monson P A 2004 *Langmuir* **20** 4289
[27] Vishnyakov A and Neimark A V 2003 *Langmuir* **19** 3240
[28] Van Der Voort P, Ravikovitch P I, De Jong K P, Benjelloun M, Van Bavel E, Janssen A H, Neimark A V, Weckhuysen B M and Vansant E F 2002 *J. Phys. Chem.* B **106** 5873
[29] Ravikovitch P I and Neimark A V 2002 *Langmuir* **18** 1550
[30] Ravikovitch P I and Neimark A V 2002 *Langmuir* **18** 9830
[31] Morishige K, Tateishi M, Hirose F and Aramaki K 2006 *Langmuir* **22** 9220
[32] Morishige K, Yasunaga H, Denoyel R and Wernert V 2007 *J. Phys. Chem.* C **111** 9488
[33] Herino R, Bomchil G, Barla K, Bertrand C and Ginoux J L 1987 *J. Electrochem. Soc.* **134** 1994
[34] Cullis A G, Canham L T and Calcott P D J 1997 *J. Appl. Phys.* **82** 909
[35] Coasne B, Grosman A, Dupont-Pavlovsky N, Ortega C and Simon M 2001 *Phys. Chem. Chem. Phys.* **3** 1196
[36] Coasne B, Grosman A, Ortega C and Simon M 2002 *Phys. Rev. Lett.* **88** 256102
[37] Valiullin R and Khokhlov A 2006 *Phys. Rev.* E **73** 051605
[38] Strange J H, Rahman M and Smith E G 1993 *Phys. Rev. Lett.* **71** 3589
[39] Valiullin R and Furo I 2002 *J. Chem. Phys.* **117** 2307
[40] Sliwinska-Bartkowiak M, Gras J, Sikorski R, Radhakrishnan R, Gelb L and Gubbins K E 1999 *Langmuir* **15** 6060
[41] Valiullin R and Furo I 2002 *Phys. Rev.* E **66** 031508